Chemical Engineering Journal 494 (2024) 153007

Contents lists available at ScienceDirect

Chemical Engineering Journal

journal homepage: www.elsevier.com/locate/cej

Generating sustainable cement material from seawater with low-cost ultrafiltration (UF) membrane electrolysis

Qian Chen, Youngwoo Choo, Nawshad Akther, Ho Kyong Shon, Gayathri Naidu *

School of Civil and Environmental Engineering, University of Technology Sydney (UTS), City Campus, Broadway, NSW 2007, Australia

ARTICLE INFO

Keywords:
Seawater
Cement production
Membrane electrolysis
Ultrafiltration membrane
Magnesium recovery
Calcium recovery

ABSTRACT

Membrane electrolysis offers a promising avenue for in-situ generation of hydroxide ions (OH^-), facilitating the recovery of magnesium (Mg^{2+}) and calcium (Ca^{2+}) ions from seawater as alkaline earth hydroxide precipitates. This process paves the way for an alternative greener method in the production of raw materials for cement manufacturing compared to limestone mining. Despite its potential, the application of conventional ion migration membranes, such as anion exchange membrane (AEM) and cation exchange membrane (CEM), is hampered by their high cost and low mechanical quality, posing significant barriers to industrial scalability. In this work, we introduce the utilization of commercially available high mechanical strength ultrafiltration (UF) membrane within a two-chamber electrochemical system, repurposing it as an ion migration membrane due to its distinct advantages in terms of simplicity and relative cost-efficiency than conventional AEM. This research demonstrates that the UF membrane exhibited a comparable performance to AEM in terms of OH^- production. Both membranes achieved 97–99 % removal of Mg^{2+} and Ca^{2+} within 3 h at a current density of 8 mA/cm^2 and maintained comparable migration rate of SO_4^{2-} ion. Compared to AEM, a notable distinction of the UF membrane is its reduced migration rate of Cl^- ions, resulting in lower membrane discoloration/oxidation. Furthermore, the investigation reveals that utilizing a Na_2SO_4 solution as an alternative anolyte, despite being slower for OH^- production, offers economic advantages and facilitates higher selective recovery of Mg^{2+} over Ca^{2+}. The end products of this process, MgO and CaO, are viable raw materials for cement production, underscoring a sustainable and low carbon approach compared to conventional limestone mining of cement production.

1. Introduction

Cement production is one of the largest contributors to global carbon dioxide (CO_2) emissions, primarily due to the calcination of limestone ($CaCO_3$) in traditional manufacturing processes, which releases significant amounts of CO_2 [1]. Portland cement, a key component of concrete and the most widely used cement type, is primarily composed of calcium oxide (CaO) (Table 1) [2]. The production of Portland cement accounts for approximately 7 % of worldwide industrial energy consumption and 8 % of carbon emissions, with CO_2 emissions resulting both from the decomposition of limestone and the combustion of fossil fuels required for high-temperature calcination [3,4]. Recent efforts to decarbonize cement production have explored various strategies, including carbon capture from flue gases, the use of supplementary cementitious materials, and the development of low-carbon alternatives such as reactive magnesia cement [5–8]. However, these approaches often face challenges related to cost, supply or performance.

Seawater membrane electrolysis using ion exchange membranes such as AEM and CEM enables efficient recovery of Mg^{2+} and Ca^{2+} ions (as alkaline hydroxide and not in carbonate form) without direct chemical addition [9], offering an opportunity for sustainable raw cement material production from seawater. For example, Pan et al. [9] demonstrated that a membrane electrolysis process equipped with a CEM and utilizing magnesium chloride ($MgCl_2$) as the anolyte achieved a substantial recovery rate of 90 % for Mg in the form of $Mg(OH)_2$. Similarly, Sano et al. [10] achieved highly effective Mg recovery (almost 99 %) in the form of $Mg(OH)_2$ by adopting a membrane electrolysis approach equipped with CEM and using Na_2SO_4 as an anolyte. In another study, Diaz Nieto et al. [11] utilized an AEM and Phosphate Buffered Saline (PBS) solution as an anolyte to process lithium-rich brines, preventing the generation of Cl_2 gas and enabling the recovery of virtually all Mg and Ca (99 %) in the form of $Mg(OH)_2$ and $Ca(OH)_2$. Despite current studies indicating that membrane electrolysis can efficiently remove Ca^{2+} and Mg^{2+} ions from seawater without direct

* Corresponding author.
E-mail address: Gayathri.Danasamy@uts.edu.au (G. Naidu).

https://doi.org/10.1016/j.cej.2024.153007
Received 11 February 2024; Received in revised form 16 May 2024; Accepted 9 June 2024
Available online 10 June 2024

Table 1
Portland cement mineralogy [4].

Materials	Cement	
Parameters	PC1	PC2
Loss on ignition (%)	1.6	1.1
IR (%)	0.7	0.1
SiO_2 (%)	19.2	21.7
Al_2O_3 (%)	6.4	1.5
Fe_2O_3 (%)	1.7	4.1
CaO (%)	63.9	68.0
MgO (%)	1.5	0.4
Na_2O (%)	0.9	0.4
K_2O (%)	0.5	0.2
SO_3 (%)	3.5	2.3
Density	3.08	3.21
Blaine (m^2/kg)	319	301

addition of chemical reagents, the potential of applying membrane electrolysis to produce cement raw material (CaO and MgO) from seawater has not been widely explored.

As a technology, seawater membrane electrolysis is attractive because firstly, using seawater to produce cement raw materials is beneficial given the natural presence of vast reservoir of carbon-free Mg and Ca at high concentrations [12] over limestone mining. Secondly, compared to membrane electrolysis, conventional chemical precipitation method for extracting Ca^{2+} and Mg^{2+} from seawater is chemically intensive and it predominantly recovers Mg^{2+} alongside Ca^{2+} and Na^{+} [12,13]. Nevertheless, one of the challenges that limit the practical application of membrane electrolysis is the high cost of AEM and CEM that is typically utilized for this process [9–11]. Apart from the high cost, AEM and CEM exhibit low mechanical strength and are susceptible to membrane damages related to oxidation (hypochlorous acid) and high alkaline conditions during seawater membrane electrolysis, restricting their long-term operational viability.

Membrane electrolysis used for hydrogen/gas production predominantly utilize AEM and CEM, as these ion exchange membranes directly influence the efficiency of selective gas/hydrogen permeation rate over ion transfer [14]. On the other hand, seawater membrane electrolysis for Ca and Mg production, theoretically, could be carried out with a simple commercial porous membrane that allows for selective cation/anion migration while more importantly, can provide a durable and robust separation barrier layer between the anolyte solution and seawater. One such relatively inexpensive robust membrane is ultrafiltration (UF) membrane. Polymeric porous UF, is widely utilized in various large-scale industrial treatment processes due to its ability to separate ions and remove macromolecules based on its pore size, cost-effectiveness, long term reusability and stability [14,15]. The cost of UF membrane such as polyethersulfone-based (PES) UF membrane (e.g., US$ 188/m^2 for the MK series of Synder Filtratio^{TM}) is approximately 80 % less expensive to AEM and CEM (US$ 333/m^2 for AMI-7001S and CMI-7000S). Also, UF membranes often exhibit superior mechanical strength due to their non-woven support layers. Considering both the reduced capital and operational expenditures, UF membranes are expected to offer better economic benefit than processes based on AEM. To date, there have been no reports on the use of UF membrane as substitutes for ion exchange membranes. Recently, Zhou et al. [16] examined the performance of seawater electrolysis using polyamide thin film composite (TFC) membrane and reported that increasing the pore size by approximately fivefold (approaching the pore size scale close to the UF membranes) had minimal impact on the transport of counterions across the membrane during electrolysis. This infers that UF membrane could be used for seawater electrolysis. Zhou et al [16] also indicated both Donnan partitioning and steric hindrance influenced the transport of co-ions to the anodic compartment with TFC membrane electrolysis [16]. In seawater electrolysis, where diffusion and electromigration predominantly govern ion transport, there is a notable scarcity of studies on the mechanisms of porous membranes such as UF membranes. It is essential to carry out studies to fill this gap and establish the suitability of applying low cost membranes such as UF membrane in seawater electrolysis. Additionally, research on the migration and diffusion behavior of ions caused by various electrolytes remains limited. While previous studies [9–11] have demonstrated effective Mg^{2+} recovery using different anolyte solutions ($MgCl_2$, Na_2SO_4, and PBS), a clear comparison of membrane electrolysis performance for separation of Mg^{2+} and Ca^{2+} in seawater with different anolyte solutions to establish an optimal solution has not been established.

Given these considerations, our study seeks to establish UF membrane electrolysis as a viable alternative method for the selective separation of Mg^{2+} and Ca^{2+} from seawater. We aim to achieve this without direct chemical additions and at low energy requirements, utilizing a cost-effective UF membrane while identifying a suitable anolyte solution. The specific objectives of our study are as follows: (1) compare the performance of AEM and UF membrane to demonstrate the applicability and feasibility of using UF membrane for the selective separation of Mg^{2+} and Ca^{2+} from seawater, elucidating the principles governing ion migration; (2) compare the performance of PBS and Na_2SO_4 anolyte; (3) selectively produce $Ca(OH)_2$ by electrolysis, which will then be converted to CaO by heating (releasing only water rather than CO_2 during production). The overarching goal of this study is to provide new insights and develop methodologies for selectively separating Mg^{2+} and Ca^{2+} from seawater to produce Portland cement raw materials in a sustainable manner.

2. Materials and methods

2.1. Membrane electrolysis setup

Commercial PES UF membrane (MK series, Synder Filtration™) and AEM (AMI-7001S, Membrane International Inc.) were purchased and used without further modification. The detailed specifications of the AEM and UF membranes are outlined in Table 2 and Table 3, respectively. Although the electrical resistance of AMI-7001S is higher than other commercially available membranes, it was chosen due to its proven stability in electrochemical systems and ability to facilitate selective ion transport, particularly with its quaternary ammonium functional group. This membrane features a homogeneous gel polystyrene structure cross-linked with divinylbenzene, which ensures uniform ion exchange and allows for efficient migration of Cl^- and SO_4^{2-} ions during electrolysis. Prior to testing the membranes, the UF membrane was immersed in ethanol for 10 mins, then rinsed and soaked in DI water for at least 24 h to ensure wettability. AEM was immersed in a 5 % sodium chloride (NaCl) solution for 12 h to ensure it was properly hydrated and swollen.

A custom made acrylic electrochemical cell was used for membrane electrolysis (Fig. S1). The cell comprised of two compartments which

Table 2
Characteristics of AEM.

Technical specification	AMI-7001S
Functionality	Strong Base Anion Exchange Membrane
Polymer Structure	Gel polystyrene cross linked with divinylbenzene
Functional Group	Quaternary Ammonium
Standard Thickness (mm)	0.45 ± 0.025
Electrical Resistance (Ω.cm^2)	<40
Maximum Current Density (A/m^2)	<500
Selectivity (%)	90
Total Exchange Capacity (meq/g)	1.3 ± 0.1
Thermal stability (°C)	90
Chemical Stability Range (pH)	1–10
Structural property	Homogeneous
Contact angle (°)	49.63
Zeta potential (mV)	+37.24 [17]

Table 3
Characteristics of UF membrane.

Technical specification	UF membrane
Membrane material	PES
pH tolerance	1–11
Flux (GFD/psi)	169–260/60
MWCO (kDa)	30
Structural property	Homogeneous
Contact angle (°)	67.83
Zeta potential (mV)	−60.5 [18]

Notes: GFD/psi is a unit of measurement used to express the permeability or flux of a filtration membrane, indicating how many gallons per day per square foot of membrane area can be filtered per pound per square inch of applied pressure; MWCO, is a term expressed in kilodaltons (kDa) and represents the approximate molecular weight of the smallest molecule that the membrane will substantially retain.

were separated by a membrane, and each compartment stores anolyte and catholyte, respectively (Fig. 1). The volume of each compartment was 500 mL. While running the experiments, a constant current density of 8 mA/cm^2 was maintained between the electrodes.

2.1.1. Electrode

A titanium (Ti) mesh electrode coated with mixed metal oxides (IrO_2/TiO_2: 65/35 %) was used as an anode, while a titanium oxide (TiO_2) mesh electrode was used as a cathode. Both electrodes were separately attached to a perpendicular current collector and each electrode had a surface area of 100 cm^2. The electrochemical experiments were conducted in a constant current mode using a potentiostat (WPG100, WonATech). The membrane electrolysis setup with anolyte solution and real seawater as the catholyte is illustrated in Fig. 1.

Due to the distinct compositions in the anodic and cathodic compartments, it can be hypothesized that water oxidizes into oxygen at the anode, as shown in Eq.(1). This process may produce intermediate reactive oxygen species and/or involve the oxidation of Cl^- to Cl_2 gas as shown in Eq.(2). Simultaneously, reduction of water to hydrogen takes place in the cathodic compartment along with the generation of OH^- as indicated by Eq.(3).

$$2H_2O \rightarrow O_2 + 4H^+ + 4e^- \quad (1)$$

$$2Cl^- \rightarrow Cl_2 + 2e^- \quad (2)$$

$$2H_2O + 2e^- \rightarrow H_2 + 2OH^- \quad (3)$$

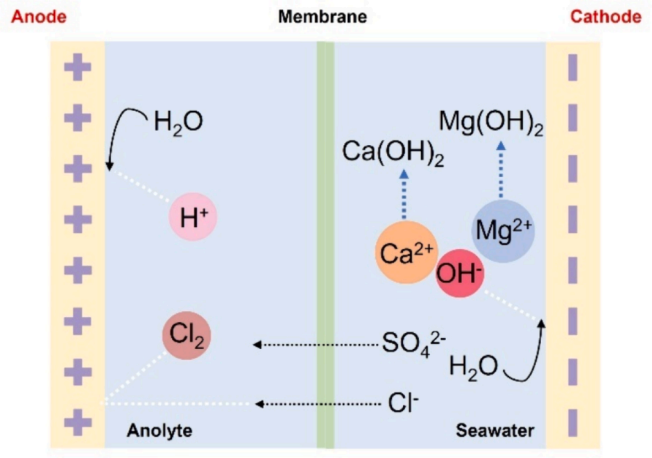

Fig. 1. Membrane electrolysis setup with anolyte solution and real seawater as catholyte.

2.1.2. Anolyte solution

Experiments were conducted using 0.1 mol/L of PBS buffer solution (consisting of 0.1 mol each of Na_2HPO_4 and NaH_2PO_4) and 0.1 mol/L of Na_2SO_4 solution as anolytes. All the chemicals used in this study were purchased from Sigma-Aldrich and were of analytical grade purity, requiring no additional treatment before use.

2.1.3. Seawater as catholyte

Seawater sourced directly from Chowder Bay in Sydney was used as catholyte. The key components of this seawater are listed in Table 4.

2.2. Membrane electrolysis process

To assess the influence of different membrane types on the overall system performance, a 0.1 mol/L PBS solution was placed in the anode chamber, while seawater was placed in the cathode chamber. A membrane was positioned between these two chambers to prevent direct contact between the two solutions. Subsequently, a current of 0.8 A (8 mA/cm^2) was applied to the system, and the experiments were terminated after 3 h. At various time intervals during this period, 1 mL samples were extracted from the cathode and anode chambers for ICP analysis to examine ion migration/diffusion behavior. Furthermore, the role of the membrane was assessed in a system, which did not include a membrane, and seawater was used as the electrolyte. To evaluate the influence of anolytes on the overall system performance, a 0.1 mol/L PBS solution and a 0.1 mol/L Na_2SO_4 solution were utilized as the anolyte, with a UF membrane serving as the barrier. All other parameters remained consistent with those mentioned previously. Moreover, the anolytes were reused for three cycles, and with each cycle, fresh seawater was introduced to evaluate the reusability of the anolytes. All experiments were conducted three times to verify the stability and repeatability of the results, and error bars were calculated based on the results and plotted accordingly.

To obtain the $Mg(OH)_2$ precipitates, we employed an electrolysis system with a 0.1 mol/L Na_2SO_4 solution as the anolyte and a UF membrane as the barrier. After running for 3 h, the treated seawater underwent filtration, and the solids were collected and dried in a 50 °C oven overnight. To produce Portland cement material, the aforementioned electrolysis system was stopped at the 2-h mark. The treated seawater was filtered to remove $Mg(OH)_2$ precipitates, and the filtered seawater was then subjected to an additional 2 h of electrolysis. After this, the solution was filtered again to yield $Ca(OH)_2$ precipitate. The filtered solids were dried in a 50 °C oven overnight and subsequently transferred to a furnace, where they were calcinated at 650 °C for 1 h to produce CaO.

Table 4
Characteristics of real seawater collected from Sydney Institute of Marine Science, Chowder Bay, Sydney, Australia.

Parameter	Value
Cations (mg/L)	
K^+	385.21 ± 0.51
Ca^{2+}	425.42 ± 0.4
Na^+	10861.13 ± 3.20
Mg^{2+}	1342.30 ± 1.61
Li^+	0.18 ± 0.03
Rb^+	0.12 ± 0.03
Sr^{2+}	8.11 ± 0.71
Anions (mg/L)	
Cl^-	20060.32 ± 3.51
SO_4^{2-}	2941.20 ± 2.21
pH	8.0 ± 0.3

2.3. Analysis

The ion concentrations of seawater before and after treatment were determined using Inductively Coupled Plasma Mass Spectrometry (ICP-MS). Additionally, the pH and the total dissolved solids (TDS) of the solution were quantified using a portable multi meter (HQ40d, Hach). The crystalline phases of the produced precipitates were examined using a Bruker D8 Discover X-ray diffractometer, employing Cu Kα radiation within the 2θ range of 5° to 50° (with a 0.04° increment) and a scan rate of 0.04°/s. Additionally, the surface morphology of both the AEM and UF membrane was investigated using a scanning electron microscopy (SEM, Zeiss Supra 55 VP). To prepare the samples for characterization, specimens were dried with wipes and further air-dried at room temperature for 12 h. Subsequently, a 10 nm thick layer of gold–palladium alloy was sputter-coated (Leica EM ACE600 High Vacuum Coater) to prevent charging effects.

3. Results and discussion

3.1. Influence of membrane on the systems performance

A typical membrane electrolysis setup employs an AEM to allow selective migration and diffusion of anions from the catholyte chamber to the anolyte chamber. This enables the cations of interest, e.g., Mg^{2+} and Ca^{2+} to remain in the catholyte chamber, thereby maximizes the recovery rate, while maintaining the total charge balance. However, the high cost limits the accessibility of the AEM-based electrolysis. Instead, we employed a UF membrane to examine if the membrane can be used as a cost-effective proxy to the AEM, potentially reducing the overall membrane expenses. We employed a 0.1 mol/L PBS solution as an anolyte, while utilizing a non-diluted seawater as a catholyte. The performance of a UF membrane in comparison to AEM was compared, aiming to substantiate its potential as a viable alternative. Alongside, the changes of anions and cations concentration in seawater was monitored to understand how the UF membrane influences ion transportation.

3.1.1. Voltage–current profile and TDS-pH trend

A time-dependent pH-TDS trend was examined to resolve the concentration of OH^- in the seawater and the extent of the transition from solvated ions to insoluble salts. Further, a time-dependent potential measurement (chronopotentiometry) was conducted to gauge the system's overall conductivity. The results are shown in Fig. 2a and b, respectively.

Fig. 2a shows the time-dependent pH and TDS trends when AEM and UF membranes were employed. In both cases, the pH of the electrolyte in the cathode side exhibited a monotonic increase. This is likely attributed to the continuous generation of OH^- (as depicted by Eq.(3)). In line with this, noticeable precipitate, appearing as a white flocculant-like particles, accumulated in the catholyte chamber.

The pH trend displays four distinct stages (Fig. 2a), which can be approximately delineated as follows: (i) increasing stage from pH 7.5–10.5 between 0–20 mins (stage I), (ii) constant stage around pH 10.5 between 20–100 mins (stage II), (iii) increasing stage from pH 10.5–13.0 between 100–140 mins (stage III), and (iv) constant stage at pH 13.0 between 140–180 mins (stage IV). Initially, the electrolysis process contributes to a consistent rise in pH over time due to the generation of OH^- ions. Upon reaching pH 10.5, the pH exhibits plateau as hydroxide ions formed insoluble alkaline earth hydroxide salts and produced white precipitates. Subsequently, there is a marked increase in pH, which continues up to approximately pH 13.0. The increase in pH indicates that the continuous water splitting occurred alongside Cl^- and SO_4^{2-} transport to the anolyte side. The TDS results showed a linear reducing trend from 0 to 100 mins, indicating that salt precipitation has occurred. In stages III and IV, the linear TDS increment corroborates the logarithmic pH increment, indicating that the presence of free hydroxide ions likely contributed to increase the TDS value.

While both AEM and UF membrane showed similar pH values, the AEM showed a slightly higher TDS reduction capacity. This could be attributed to the higher Cl^- transport capacity of AEM (Table 5). Specifically, 54 % Cl^- ion reduction occurred with AEM, while UF membrane achieved only around 27 % Cl^- ions reduction. This is evidently

Table 5
Comparison of anion transportation over time for AEM and UF membrane (mg/L).

Membrane type	Elements	0 min	60 min	120 min	180 min
AEM	Cl^-	20060.3 ± 3.5	17693.1 ± 4.0	15288.2 ± 3.9	9183.5 ± 4.7
	SO_4^{2-}	2941.2 ± 2.2	2678.4 ± 2.8	2522.0 ± 2.5	2030.2 ± 3.1
UF	Cl^-	20060.3 ± 3.5	17722.3 ± 4.2	16199.1 ± 3.8	14737.7 ± 2.8
	SO_4^{2-}	2941.2 ± 2.2	2494.0 ± 1.8	2349.5 ± 2.3	2212.1 ± 3.1

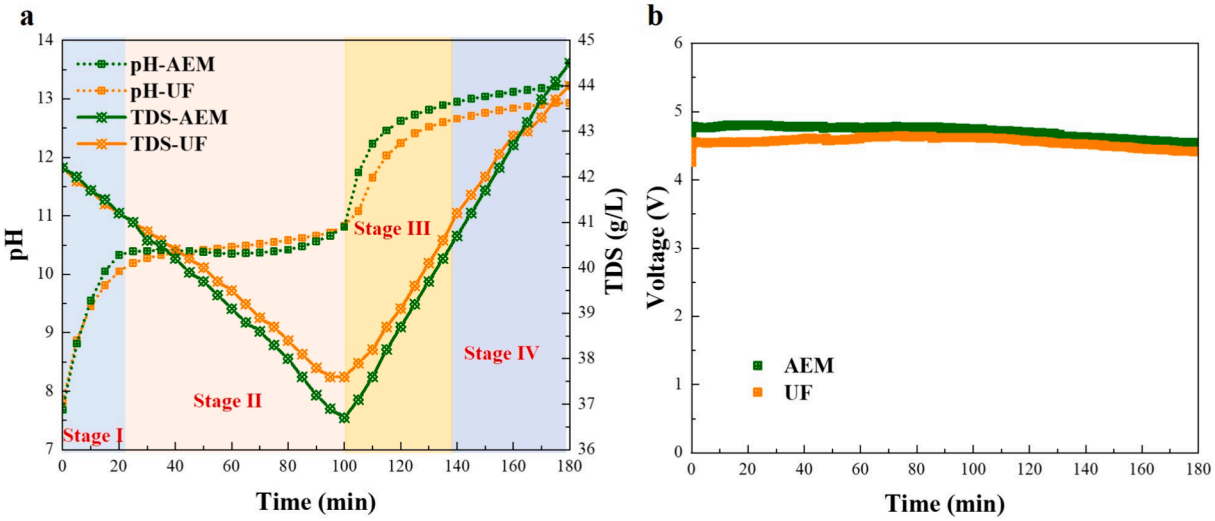

Fig. 2. (a) Correlation of pH-TDS trends with time and (b) voltage–time relationship for UF membrane and AEM in 0.1 mol/L PBS solution (Constant current: 8 mA/cm^2).

because AMI-7001S AEM is tailored as a Cl^- exchange membrane, modified with quaternary ammonium functional groups, exhibiting a Cl^- selectivity exceeding 90 %. Additionally, the surface potential of the AEM is + 37.24 mV, while that of the UF membrane is −60.5 mV, indicating a stronger electrostatic attraction of AEM for anions [17,18]. Consequently, this membrane displays a pronounced affinity for facilitating the transport of Cl^- ions from the cathode to the anode side. Meanwhile, the UF membrane performs as a non-selective semipermeable barrier, allowing the transport of both Cl^- and SO_4^{2-} through the membrane pores. This is primarily driven by electrostatic attraction to the positively charged anode electrode and this driven force is significantly stronger than the electrostatic repulsion provided by the UF membrane's own negative potential against anions. The overall anion transport through the UF membrane appears similar in both Cl^- and SO_4^{2-} (27 and 25 %, respectively) and relatively lower than that observed with the AEM (54 and 31 %, respectively, Table 5). This discrepancy can be attributed to the inherent selective property of AEM, which has higher electrostatic/chemical affinity toward anions, facilitating their enhanced *trans*-membrane transport.

We observed that the potential across the electrodes measured over time overlaps for both AEM and UF membrane, demonstrating that the conductivity was maintained regardless of the membrane types (Fig. 2b).

To understand the role of membrane as a barrier layer and Cl^- transportation, an electrolytic cell without a separation membrane (membrane-less) [19] was employed while seawater was used as an electrolyte. The pH-TDS trend (Fig. S2) clearly shows minimal changes to pH and TDS value. The overall pH value consistently remains below 8.0, ultimately indicating a weakly acidic condition. This suggests that oxygen evolution reaction (Eq.(1)) dominates at the anode side and thus the proton is produced. Additionally, the TDS value remains constant during the electrolysis, indicating a significant inhibition of salt precipitation due to the low pH value. Regarding the voltage trend depicted in Fig. S2, it maintains a consistent behavior over time, comparable to the voltage presented in Fig. 2b. Based on the pH-TDS and voltage–time trends observed in the membrane-less system, this process is not conducive to the formation of alkaline earth hydroxide precipitates and thus, the separation membrane plays a critical role in the production of OH^- and precipitates.

3.1.2. *Mg recovery rate and other major cations in seawater*

The time-dependent cation concentration of Mg^{2+}, Ca^{2+}, Na^+ and K^+ was studied to investigate the formation of precipitates (Fig. 3).

Fig. 3a illustrates a linear reduction in the concentration of Mg^{2+} ions within the first 100 mins. Remarkably, both UF membrane and AEM showcase similar removal rate of Mg^{2+}. Conversely, the trend for Ca^{2+} ions show non-linear decreasing trend, similar to the logarithmic decay curve (Fig. 3b). It is imperative to highlight that the AEM consistently displayed a higher Ca^{2+} concentration than that of UF membrane during the test. This indicates a more efficient removal rate of Ca^{2+} ions when employing the UF membrane. Specifically, within the first 100 mins, the UF membrane facilitated the removal of approximately 52 % of Ca^{2+}

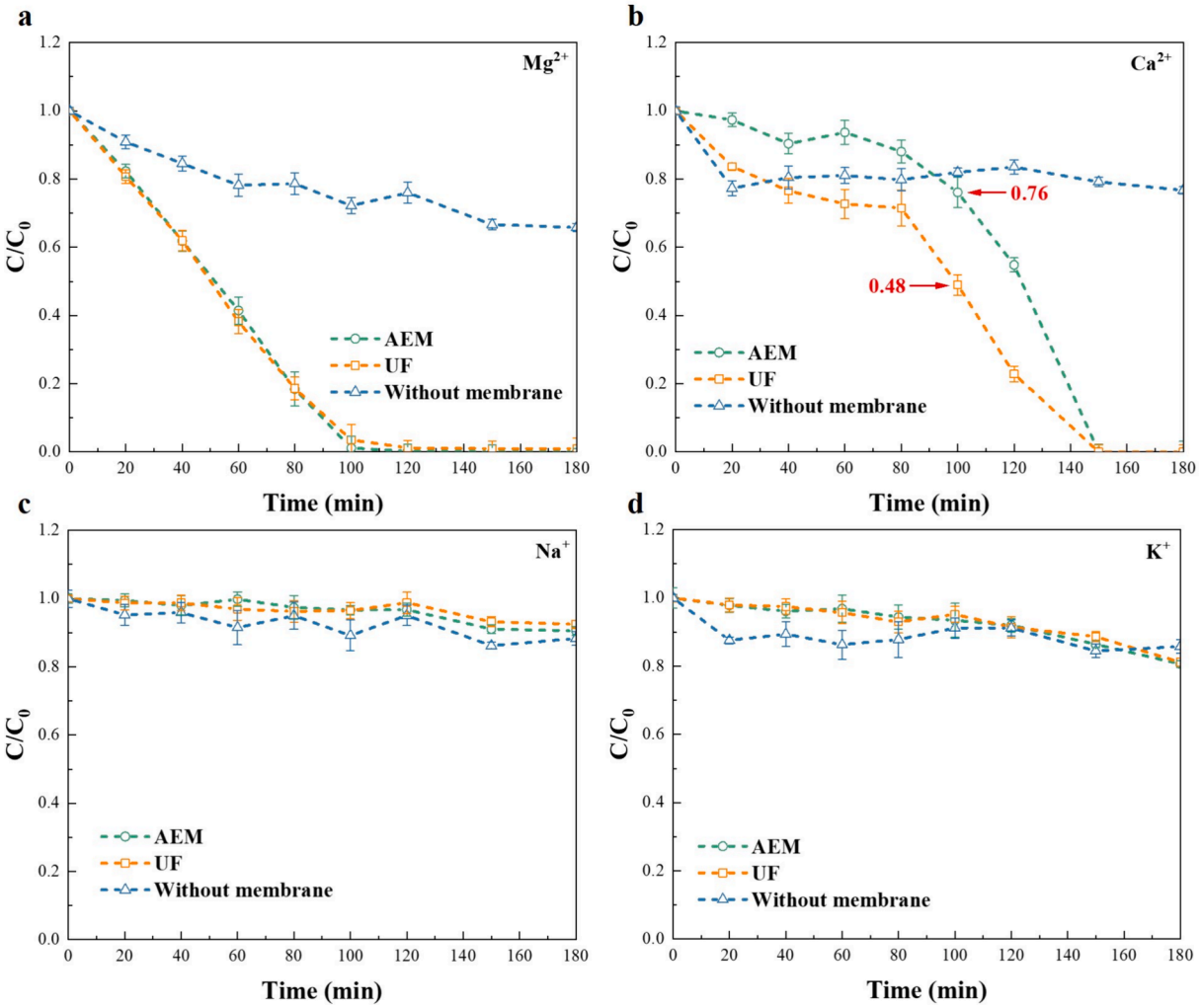

Fig. 3. Concentrations of (a) Mg^{2+}, (b) Ca^{2+}, (c) Na^+ and (d) K^+ for UF membrane and AEM in 0.1 mol/L PBS solution (constant current: 8 mA/cm^2).

ions, contrasting to a mere 24 % removal when the AEM was used. The capacity to generate OH^- is equivalent for both the AEM and the UF membrane, as depicted in Fig. 2a. However, it is noteworthy that the removal of Ca^{2+} varies significantly between the two membranes, underscoring the role of membrane type in governing the migration behaviors of ions within the solution, consequently influencing salt precipitation of Ca^{2+}.

As for the Na^+ and K^+ ions (Fig. 3c and d), their concentrations remain relatively stable throughout the process. However, a slight reduction in both ions is observed after the 100 mins mark, likely due to adsorption onto the negatively charged precipitates.

In addition to monitoring the changes in concentrations of various cations on the cathode chamber, the changes in cation concentrations in the anolyte were also measured to observe the overall ion migration behavior, as shown in Table 6. The table indicates that, for both AEM and UF membranes, the concentrations of cations such as K^+, Mg^{2+}, and Ca^{2+} increased, while the concentration of Na^+ ions decreased. This is because to balance the overall charges, some cations from the seawater diffused to the anode side. The reduction of Na^+ ions on the anode side is due to the electrostatic attraction of the cathode electrode. When using both types of membranes, the final mass of precipitate produced was comparable, with 2.06 g for the AEM and 2.08 g for the UF membrane. The results suggest the rate of cation removal using the UF membrane is comparable to that achieved with the AEM. Furthermore, the anions like Cl^- and SO_4^{2-} ions migrate to the anode side and partake in other side reactions, e.g., chlorine evolution reaction, which subsequently influencing the overall electrolysis performance.

The residual concentrations of Mg^{2+}, Ca^{2+}, Na^+, and K^+ in seawater within the membrane-less system [19] is also depicted in Fig. 3. It is evident that over 60 % of Mg^{2+} remains in the solution (Fig. 3a), while the concentration gradually decreases. Approximately 20 % of Ca^{2+} was initially removed within the first 20 mins, after which it stabilizes at around 80 % (Fig. 3b). The concentrations of Mg^{2+} and Ca^{2+} in the membrane-less system is notably higher than those in the membrane-assisted system. This difference arises because the membrane plays a crucial role in creating a barrier that inhibits the reaction between H^+ and OH^-. Consequently, the OH^- ions sequestered in anode compartment are more susceptible to form insoluble alkaline earth hydroxide precipitates.

Combined with the results of pH and TDS (Fig. 2a), the white precipitates are producing within 100 mins. Mg^{2+} and Ca^{2+} both have the potential to precipitate as their respective hydroxides, $Mg(OH)_2$ and $Ca(OH)_2$ (Eq.(4) and Eq.(5)). According to their solubility products ($K_{sp,\ Mg(OH)2} = 1.8 \times 10^{-11}$ and $K_{sp,\ Ca(OH)2} = 5.5 \times 10^{-6}$, at 25 °C) [10], the precipitation of $Mg(OH)_2$ should precede that of $Ca(OH)_2$. As shown in Fig. 4, the species distribution diagrams of Mg^{2+} and Ca^{2+} demonstrate that the Mg^{2+} ions precipitate as $Mg(OH)_2$ when pH reaches 8.8, whereas the Ca^{2+} ions precipitates above pH 12.4. This observation suggests that $Mg(OH)_2$ precipitates are the principal products formed within the initial 100 mins electrolysis period. These findings are consistent with the trend in pH and TDS values, as well as the observed changes in ion concentrations. Furthermore, the results demonstrate that membrane electrolysis is capable of facilitating the recovery of Mg^{2+} and Ca^{2+} from seawater, converting them into $Mg(OH)_2$ and $Ca(OH)_2$. By precisely tuning the reaction time and consequently the pH of the catholyte solution, we can selectively separate Mg^{2+} and Ca^{2+} in the seawater.

$$Mg^{2+}(aq) + 2OH^-(aq) \rightleftharpoons Mg(OH)_2(s) \quad (4)$$

$$Ca^{2+}(aq) + 2OH^-(aq) \rightleftharpoons Ca(OH)_2(s) \quad (5)$$

Table 6
Comparison on the mass of migrated/diffused cations at the anode chamber using AEM and UF membrane in 0.1 mol/L PBS solution.

Membrane	Ion migration in mass, mg				Mass of precipitates, g
	K^+	Na^+	Mg^{2+}	Ca^{2+}	
AEM	2.5 ± 0.5	−334.2 ± 2.1	0.8 ± 0.2	2.6 ± 0.5	2.06
UF	3.0 ± 0.4	−251.5 ± 2.4	7.4 ± 1.5	1.6 ± 0.3	2.08

3.1.3. Analysis of used AEM and UF membrane

The surface of virgin/unused AEM and UF membrane are visibly smooth (Fig. S3). Following the electrolysis process, it is evident that the surface morphology of both membranes remains unchanged. The results indicate that in a short-term condition (one cycle), both UF and AEM exhibited insignificant fouling development. Therefore, to investigate the fouling development, and reuse capacity of AEM and UF membranes, experiments were carried out three times using the same membrane. From Fig. S4 it is evident that after three repeated membrane usage, the surface of both AEM and UF membranes shows membrane discoloration (brown/yellow stains on the membrane surface). This discoloration is likely due to the formation of strong oxidizing agents from the oxidation of chloride ions. In contrast, only minor oxidation was visible on the UF membrane's surface (minimal discoloration/stains observed), likely because the UF membrane allows fewer chloride ions to pass through, resulting in a lighter degree of chloride ion oxidation. To validate the long-term viability of the UF membrane to the seawater electrolysis, we performed SEM characterization of the membrane surface facing to the seawater compartment after 3 cycles of reuse. As shown in Fig. S5, minor presence of salt/precipitates was detected on the UF membrane. It is likely that salt adhered onto the membrane surface and did not result in severe scaling/pore blocking as the process performance was similar with reused membrane. The surface of AEM showed no obvious signs of salt deposition/scaling. This is likely due to the absence of the hydrodynamic flow across the membrane and the high positive charge density of AEM membrane.

3.2. Influence of anolyte solution on the systems performance

Conventionally, PBS solution is often utilized for brine electrolysis as it effectively prevents the oxidation of Cl^- to Cl_2 gas at the anode side. However, due to its high cost, its preference is waning in comparison to other anolytes such as $MgCl_2$ and Na_2SO_4. Notably, the cost of Na_2SO_4 is orders of magnitude lower than that of $MgCl_2$ and PBS, positioning it as a potential economical alternative. Consequently, this study compared the overall performance of membrane electrolysis using a UF membrane in 0.1 mol/L PBS solution to that in 0.1 mol/L Na_2SO_4 solution to ascertain the economic feasibility and applicability of Na_2SO_4 as a replacement for PBS.

The influence of anolyte solutions (0.1 mol/L of PBS buffer solution and 0.1 mol/L of Na_2SO_4 solution) on the overall performance of the system was evaluated by comparing the pH-TDS trend, the voltage profile, and the recovery rate of Mg and other major ions from seawater.

3.2.1. TDS-pH trend and voltage-current profile

As illustrated in Fig. 5a, the initial pH increment trend during stage I (0–20 mins) exhibits a significant overlap irrespective of the anolyte utilized, thereby indicating that the predominant reaction occurring at the anode side during this phase is the oxidation of H_2O, accompanied by the generation of H^+ ions and O_2 gas. This reaction facilitates the release of four electrons. Nevertheless, it is noteworthy that the duration of stage II was extended to 20–120 mins for the Na_2SO_4 solution, in contrast to the 20–100 mins for the PBS solution. Moreover, a pronounced difference in pH levels during stage III between the PBS and Na_2SO_4 solutions is observed.

This can be attributed to the inability of the Na_2SO_4 solution to assimilate the produced H^+ ions, fostering an acidic environment that facilitates the oxidation of Cl^- ions to Cl_2 gas (Eq.(3)). Unlike PBS buffer, where the pH remains consistent at approximately 7.0, the pH of the

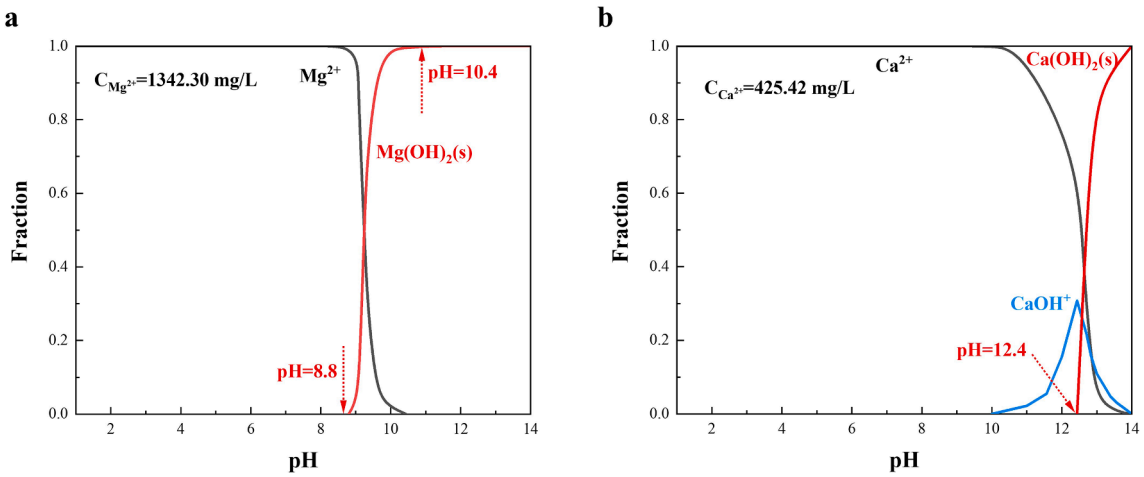

Fig. 4. Distribution diagrams of (a) 1358 mg/L of Mg^{2+} and (b) 440 mg/L of Ca^{2+} as functions of pH values.

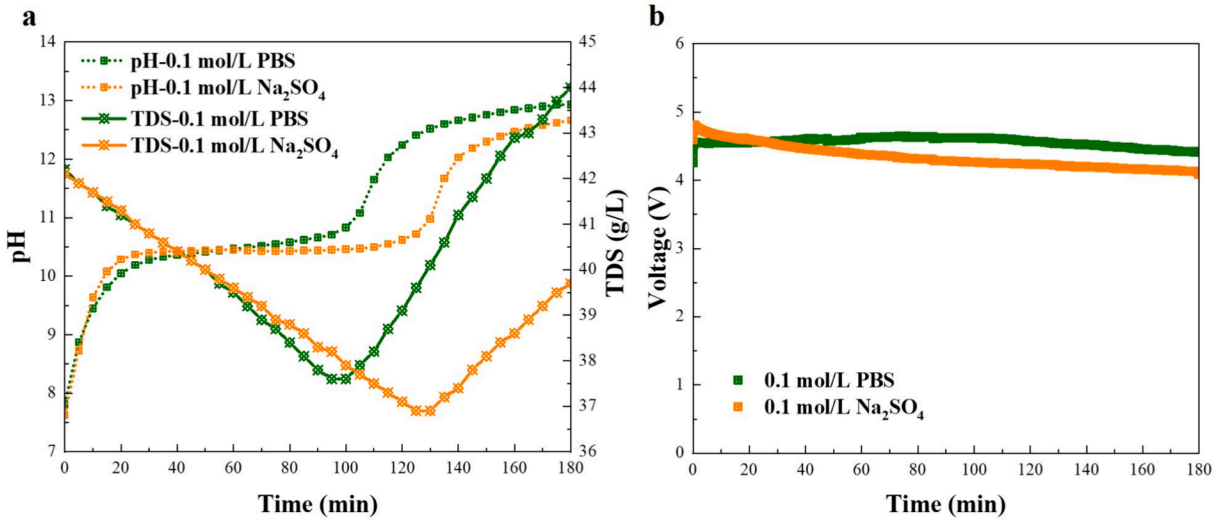

Fig. 5. (a) Correlation of pH-TDS trends with time and (b) voltage–time relationship for UF membrane in 0.1 mol/L Na_2SO_4 and 0.1 mol/L PBS solution (constant current: 8 mA/cm^2).

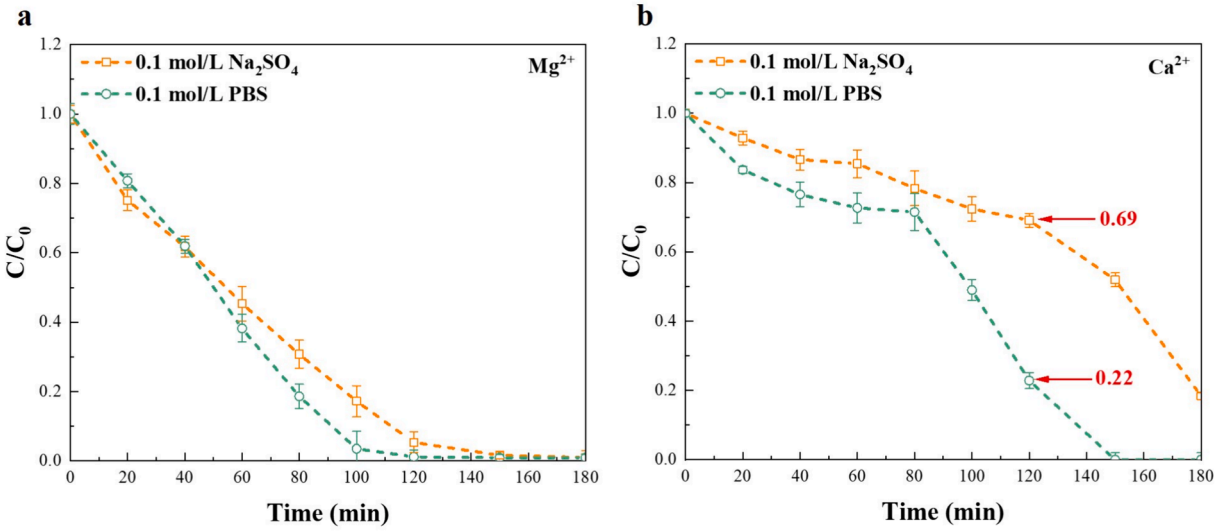

Fig. 6. Concentrations of (a) Mg^{2+} and (b) Ca^{2+} for UF membrane in 0.1 mol/L Na_2SO_4 solution and 0.1 mol/L PBS solution (constant current: 8 mA/cm^2).

Na_2SO_4 solution changes during the water splitting reaction as protons are produced at the anode. Consequently, the Cl^- ions migrated from the cathode side are more prone to oxidation compared to H_2O, given their lower standard electrode potential, a process that releases two electrons. This mitigated electron release subsequently impacts the reduction of H_2O at the cathode side, consequently lowering the concentration of generated OH^- ions.

As depicted in Fig. 5b, the voltage trend for both Na_2SO_4 solution and PBS solution is comparable over the time tested, demonstrating that the anolyte types have a negligible effect on the conductivity of the overall system.

3.2.2. Mg^{2+} And Ca^{2+} recovery rate and difference

As illustrated in Fig. 6a, utilizing 0.1 mol/L of PBS solution as anolyte results in a linear decrease in Mg^{2+} ion concentration, achieving nearly complete removal from the seawater after 100 mins of operation. In contrast, employing 0.1 mol/L Na_2SO_4 solution delays the complete removal of Mg^{2+} to 120 mins, which aligns well with pH behavior. Similarly, the Ca^{2+} concentration decreased more steadily with 0.1 mol/L Na_2SO_4 solution. Interestingly, the decreasing trend of the Ca^{2+} concentration was more pronounced with 0.1 mol/L Na_2SO_4 solution than with 0.1 mol/L PBS solution. This result suggests that, compared to the PBS solution, utilizing Na_2SO_4 solution holds promise for the selective precipitation of Mg^{2+} ions, leaving a majority of Ca^{2+} ions to remain in the solution. The selectivity of Mg^{2+}-Ca^{2+} separation was investigated by calculating the recovery difference, as shown in Table 7. Using a 0.1 mol/L PBS solution, the recovery difference for $Mg^{2+}$and Ca^{2+} reached its maximum value of 34.4 % after 60 mins of operation. However, 38.2 % of Mg^{2+} ions remained in the seawater, indicating insufficient recovery of the Mg^{2+}resource and resulting in wastage. In contrast, when using a 0.1 mol/L Na_2SO_4 solution, the maximum recovery difference reached 63.8 % after 120 mins of operation. Only 5.3 % of Mg^{2+} ions were not recovered, while approximately 70 % of Ca^{2+} remained in the seawater, which is advantageous for the production of Portland cement material. This demonstrates a greater selectivity for Mg^{2+}-Ca^{2+} separation with the Na_2SO_4 solution. Furthermore, compared to the 2.08 g of precipitate produced using the PBS anolyte, the Na_2SO_4 anolyte yielded approximately 0.5 g less (1.52 g). This underscores the Na_2SO_4 anolyte's enhanced selectivity for separating Ca^{2+} and Mg^{2+} ions, as a greater amount of Ca^{2+} ions remained un-crystallized in the seawater.

Table 7
Ca^{2+} and Mg^{2+} concentration in seawater treated with UF membrane electrolysis in 0.1 mol/L Na_2SO_4 solution and 0.1 mol/L PBS solution.

Anolyte	Elements	Original seawater (mg/L)	Time, min			
			20	60	120	180
PBS	Mg^{2+}	1342.3	1084.0	512.9	15.6	12.5
	Mg^{2+} recovery, %	-	19.2	61.8	98.8	99
	Ca^{2+}	425.4	355.6	309.0	97.1	0
	Ca^{2+} recovery, %	-	16.4	27.4	77.2	100
	Δ Mg^{2+} -Ca^{2+} Recovery, %	-	2.8	34.4	21.6	−1.0
Na_2SO_4	Mg^{2+}	1342.3	1008.0	608.5	71.6	13.4
	Mg^{2+} recovery, %	-	24.9	54.7	94.7	99.0
	Ca^{2+}	425.4	394.7	363.1	293.8	78.1
	Ca^{2+} recovery, %	-	7.2	14.6	30.9	81.6
	Δ Mg^{2+} –Ca^{2+} Recovery, %	-	17.7	40.1	63.8	17.4

*Note: Mg^{2+} recovery=$(C_{Mg(i)}-C_{Mg(t)})/C_{Mg(i)}$; Ca^{2+} recovery=$(C_{Ca(i)}-C_{Ca(t)})/C_{Ca(i)}$. $C_{Mg(t)}$ and $C_{Ca(t)}$ represent the concentration of Mg^{2+} and Ca^{2+} at specific time; $C_{Mg(i)}$ and $C_{Ca(i)}$ represent the initial concentration of Mg^{2+} and Ca^{2+} in seawater. Δ Mg^{2+}-Ca^{2+} Recovery = Mg^{2+} recovery- Ca^{2+} recovery.

3.2.3. Recovery rate of other major ions

The concentrations of K^+ and Na^+ ions marginally decreased throughout the electrolysis process, as shown in Fig. 7a and b. Following 140 mins, a slight reduction in Na^+ and K^+ concentration was observed with a 0.1 mol/L PBS solution. This can primarily be attributed to the high pH of the solution exceeding 12.4 beyond this point [20]. Notably, this reduction in monovalent ion concentrations was not observed with a 0.1 mol/L Na_2SO_4 solution, as the pH value of the seawater did not reach 12.4 during the experiment. Given that the isoelectric point for $Mg(OH)_2$ is 12.4, the precipitated $Mg(OH)_2$ takes on a negative charge at this juncture. Consequently, there exists an electrostatic attraction between the negatively charged $Mg(OH)_2$ precipitate and the cations present within the solution [21].

Based on the pH-TDS trend, voltage–time curve, and the concentration change of cations, it can be concluded that Na_2SO_4 solution has potential as a viable alternative to PBS solution as an anolyte in seawater electrolysis processes, especially given its analogous efficacy in selectively separating Mg^{2+} and Ca^{2+} ions. The primary benefits of adopting Na_2SO_4 solution are delineated by its markedly reduced cost in comparison to PBS solution, coupled with its selective capability in facilitating the recovery of Mg^{2+} ions over Ca^{2+} ions.

3.3. Reusability of PBS and Na_2SO_4 anolytes

The reusability of anolyte is also an imperative parameter to determine its economic viability and practicability. Three cycles of both anolytes, 0.1 mol/L of PBS and 0.1 mol/L of Na_2SO_4, were tested with UF membrane and the results are shown in Fig. 8.

When using 0.1 mol/L Na_2SO_4 as the anolyte, the concentration of Mg^{2+} ions (Fig. 8a) showed a slower decreasing behavior in the second cycle (2C) than in the first. In the first cycle (1C), Mg^{2+} ions achieved ~95 % removal rate within 120 mins while it took 180 mins in the second cycle (2C). In the third cycle (3C), the Mg^{2+} ion reduction curve almost coincided with the 2C. The pH of Na_2SO_4 is expected to substantially reduced after the first cycle due to the water electrolysis reaction (Eq.(1)) in the anode side during the first cycle (1C). Consequently, the competing chlorine evolution reaction (Eq.(2)) likely to occur more favorably in the following cycles because of the acidic environment. The yellowing of the Na_2SO_4 solution after use indicates the oxidation of Cl^- ions (Fig. S6). As a result, the number of electrons received on the cathode side decrease, accordingly, affecting the production of OH^- ions on the cathode side, which in turn slows down the removal rate of Mg^{2+} ions. The Ca^{2+} removal rate shows a different trend to that of Mg^{2+} (Fig. 8c). In the 1C, only 20 % of the Ca^{2+} remained in the solution after 180 mins. In the 2C, a moderate amount of Ca^{2+} was removed, with 60 % of the Ca^{2+} ions still present in the solution after 180 mins. In the 3C, 90 % of the Ca^{2+} ions remained in the solution after 180 mins. The results indicate that during the 2C, the oxidation of Cl^- occurred concurrently with the water electrolysis. During the 3C, the oxidation of Cl^- dominated, resulting in insufficient OH^- production and thus the pH did not increase sufficiently for Ca^{2+} to precipitate.

When employing a 0.1 mol/L PBS as the anolyte, more than 95 % of Mg^{2+} ions were removed within 100 mins during the 1C (Fig. 8b). In the 2C, a comparable level of Mg^{2+} ion removal was achieved in 120 mins, indicating that the PBS solution has recycling capability after two cycles. In the 3C, it required 180 mins to achieve a 95 % removal rate for Mg^{2+} ions. The stable performance in the first two cycles is attributed to the buffering effect of PBS solution, which can be demonstrated from the solution color that remained similar after use (Fig. S6). However, in the 3C, the PBS solution experienced substantial dilution in the preceding two consecutive cycles, and the partitioning of the chloride ions into the anolyte solution hampered H^+ production rate. Consequently, there was a decreased generation of OH^- ions on the cathode side, causing a delay in the removal of Mg^{2+} ions. The removal of Ca^{2+} ions took 150–180 mins, showing no significant difference. For both Na^+ and K^+ ions (Fig. S7), the concentration remains relatively stable, exhibiting no

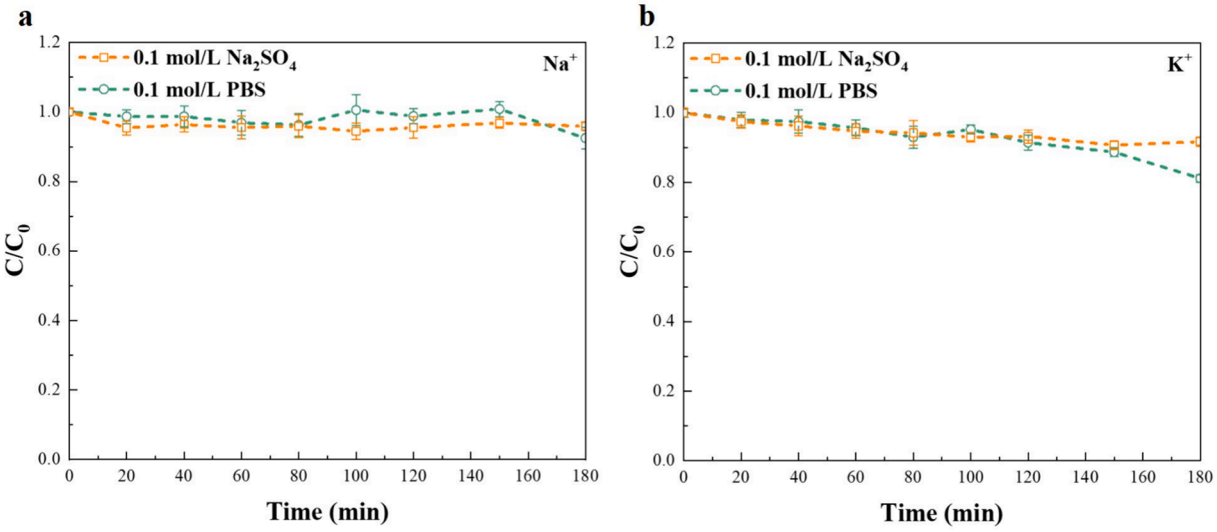

Fig. 7. Concentrations of (a) Na^+ and (b) K^+ for UF membrane in 0.1 mol/L Na_2SO_4 solution and 0.1 mol/L PBS solution (constant current: 8 mA/cm^2).

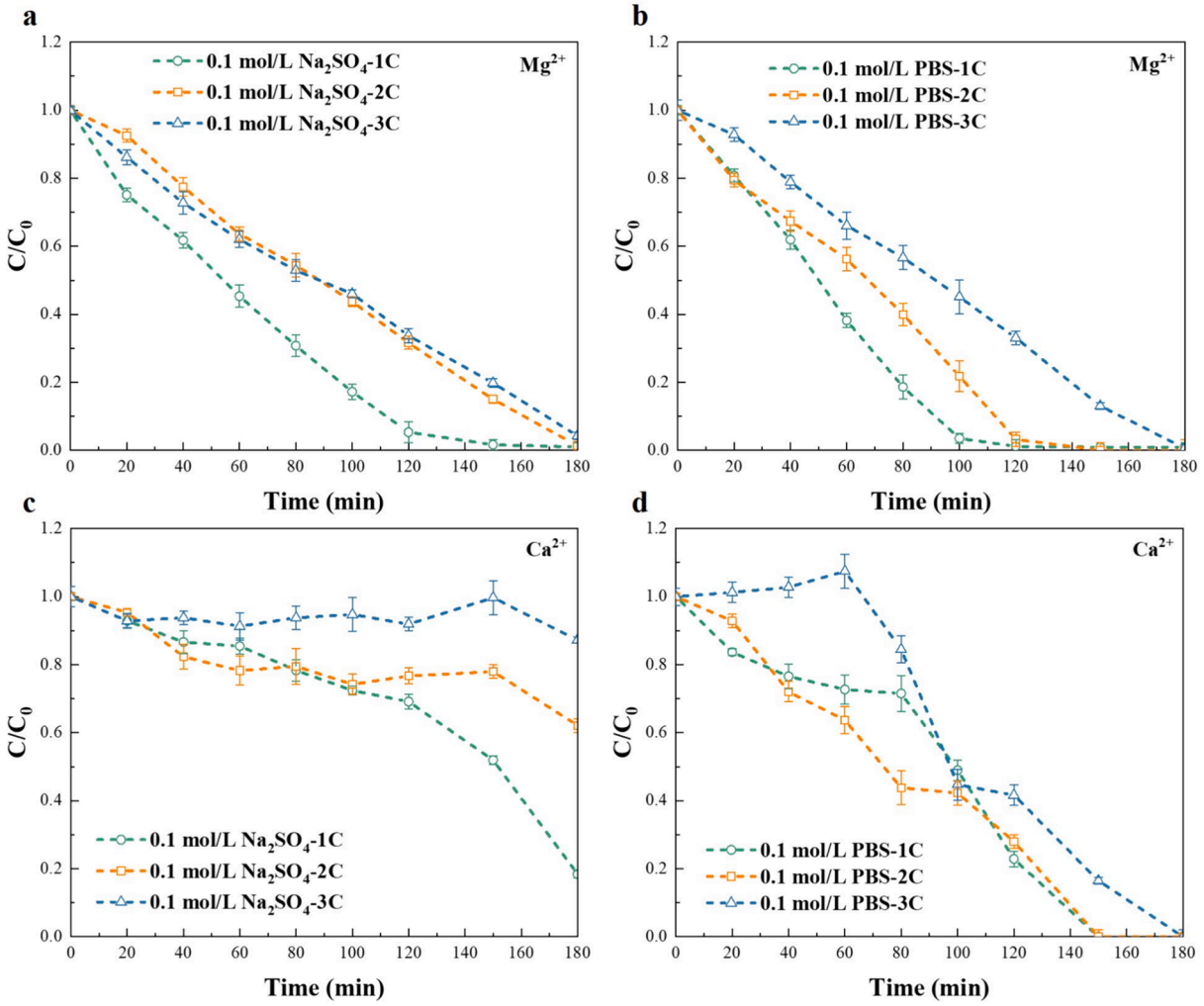

Fig. 8. Effect of reuse cycles of anolytes on the concentration of Mg^{2+} and Ca^{2+}; (a) and (c): the concentration of Mg^{2+} and Ca^{2+} concentrations with 0.1 mol/L Na_2SO_4 solution, respectively; (b) and (d): the concentration of Mg^{2+} and Ca^{2+} with 0.1 mol/L PBS solution (UF membrane, constant current density: 8 mA/cm^2).

significant fluctuations after multiple cycles, regardless of the anolyte used.

When using PBS and Na_2SO_4 as electrolytes, the changes in the concentrations of K^+, Na^+, Mg^{2+}, and Ca^{2+} ions at the anode side were essentially the same (Table S1). A small difference was noted in the mass of the precipitate formed. Compared to the PBS electrolyte, the precipitate mass produced using the Na_2SO_4 electrolyte was about 0.5 g less, which is attributed to the higher selectivity of the Na_2SO_4 electrolyte. However, clear solution color change was observed with Na_2SO_4 solution turning yellow after use (Fig S6), indicating oxidation of chloride ions, consistent with our hypothesis. Similar mass of cation diffusion was observed for all three cycles. Anolyte solution reuse marginally affected mass cation diffusion. The main factor that anolyte solution reuse affected was Ca^{2+} and Mg^{2+} separation efficiency as described in Fig. 8. Due to this, the quality of the precipitates is compromised slightly, specifically, when using PBS, after three cycles, the final product mass decreased successively from 2.08 g to 1.93 g. However, when using Na_2SO_4, the final product mass decreased from 1.52 g to 1.21 g. The main reason for this decline in product mass is the increasing participation of chloride ions in the oxidation reaction, leading to a gradual decrease in the concentration of hydroxide ions generated, thereby affecting the final product mass.

It follows that the efficacy of the Na_2SO_4 solution in removing Mg^{2+} is marginally inferior to that of the PBS solution. However, this slight decrement in efficiency can be offset by its more economical cost. Significantly, the Na_2SO_4 solution exhibits enhanced selectivity for Mg^{2+}, which is advantageous for the production of $Mg(OH)_2$ with a higher purity.

3.4. Detail composition of ED treated seawater

Table 8 presents a comparison of the concentrations of Li^+, Rb^+, Na^+, Mg^{2+}, K^+ and Ca^{2+} ions in seawater after electrolysis using a 0.1 mol/L Na_2SO_4 solution with a UF membrane. The concentrations of Li^+ and Rb^+ ions remain relatively stable throughout the 3 h treatment (~0.2 mg/L and ~0.1 mg/L, respectively). However, the concentration of Mg^{2+} ions decreased from 1342.3 mg/L to 13.4 mg/L after 3 h treatment, suggesting that 99 % of the Mg^{2+} ions were removed. Concurrently, the concentration of Ca^{2+} ions in seawater decreased by 82 %. The removal of Mg^{2+} and Ca^{2+} ions and the retention of Li^+ ions is attributed to the substantially lower solubility product constant (K_{sp}) of $Mg(OH)_2$ and $Ca(OH)_2$, allowing them to form precipitates while the Li^+ and Rb^+ ions remain hydrated.

In the context of Li^+ recovery from seawater using hydrogen manganese oxide (HMO) as Li ion exchange nanomaterial, the presence of Mg^{2+} ions significantly impede efficiency due to their comparable physicochemical properties, i.e., ionic radii [13,22]. However, through membrane electrolysis, Mg^{2+} ions can be preemptively eliminated, exerting a minimal impact on Li^+ ions. This paves the way for an enhanced recovery rate of Li^+ from seawater. Crucially, the membrane electrolysis process elevates the pH from approximately 8.0 to levels nearing 13.0 (Table 6), thereby creating a satisfactory environment conducive to HMO ion-exchange.

3.5. Mg salt production

Fig. S8 presents the seawater samples before and after membrane electrolysis, with subsequent collection of the white precipitates generated in the process. These precipitates underwent filtration, drying and were analyzed using powder XRD to identify the product. This analysis aimed to affirm the feasibility of using the UF membrane and Na_2SO_4 solution for the recovery of $Mg(OH)_2$ from seawater through the membrane electrolysis process.

The XRD pattern of the resultant solid precipitate is presented in Fig. 9, revealing characteristic peaks corresponding to $Mg(OH)_2$ [JCPDS No. 7-0239]. These peaks, observed at 2θ positions of 18.6°, 33.1°, 38.2° and 51.0°correspond to the (001), (100), (101) and (102) crystallographic planes, respectively, providing clear evidence of the presence of $Mg(OH)_2$. In addition to these discernible peaks, the characteristic peaks of NaCl are also evident, along with minor unidentified peaks. The presence of soluble NaCl salts suggests potential nucleation during the filtration and drying processes. While $Mg(OH)_2$ serves as a raw material for manufacturing MgO-based cement, a comprehensive chemical analysis is essential to determine the weight percentage of each component, a step not undertaken in the current study. Such analysis

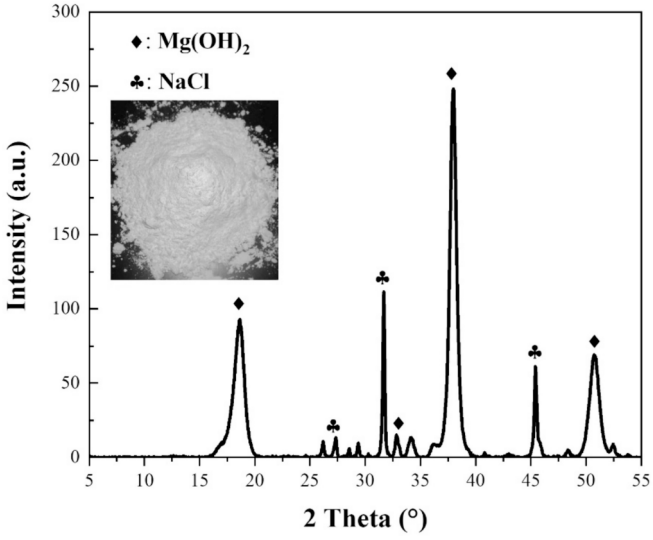

Fig. 9. XRD patterns of final products after membrane electrolysis.

Table 8
The ions concentration of seawater treated with UF membrane electrolysis in 0.1 mol/L Na_2SO_4 solution.

Seawater characteristics	Element	Original seawater	ED treated seawater, mins			
			20	60	120	180
Major cations (mg/L)	Na^+	10861.1	10368.0	10374.5	10355.3	10415.8
	Mg^{2+}	1342.3	1008.0	608.5	71.6	13.4
	K^+	385.2	381.1	370.3	364.4	358.5
	Ca^{2+}	425.4	394.7	363.1	293.8	78.1
Minor cations (mg/L)	Li^+	0.2	0.2	0.2	0.2	0.2
	Rb^+	0.1	0.1	0.1	0.1	0.1
pH		8.0	10.0	10.4	12.2	12.9
TDS		42.2	41.2	39.5	39.1	44.0

would provide a deeper understanding of the material composition and refine the feasibility assessment of UF membrane and Na_2SO_4 solution in recovering $Mg(OH)_2$ from seawater through membrane electrolysis..

3.6. Ca recovery for sustainable cement production

Operating at a current density of 0.8 mA/cm^2, after the removal of Mg^{2+} ions within the initial 2 h period, the system continued to run for an additional 120 mins to selectively recover Ca^{2+} from the seawater. The resulting Ca-containing precipitate was subjected to DI water washing to eliminate soluble impurities and dried overnight. Subsequently, the resulting solids were transferred to a furnace for calcination, completing the preparation of the raw material.

By analyzing the XRD patterns presented in Fig. 10, it is clear that the prominent characteristic peaks align with CaO, as evidenced by the 2θ peaks at 32.3°, 37.4°, and 54.0°, corresponding to the (1 1 1), (2 0 0), and (2 2 0) lattice planes. Furthermore, the elemental composition revealed by SEM-EDS elemental analysis (Fig. S9) shows the following: O (45.1 wt %), Ca (34.7 wt%), Mg (10.4 wt%), and C (9.1 wt%), with trace amounts of Na, Cl, and S. These findings corroborate that the majority of the precipitate consists of CaO, which is in accordance with the observation by XRD. As mentioned (Table 1), CaO is the main ingredient for cement production. This observation demonstrates the successful generation of raw materials essential for cement production, specifically CaO, without the formation of their carbonate compounds. This approach offers a pathway to significantly mitigate CO_2 emissions during the cement manufacturing process.

The capacity to produce CaO (the dominant ingredient for cement production) from seawater using the low cost UF membrane electrolysis method we developed is of high significance. This is because most other available methods do not effectively separate Ca from Mg in seawater. For instance, nanofiltration (NF) can effectively recover both Ca and Mg from monovalent ions in seawater, but do not separately recover Ca from Mg [23]. Moreover, to achieve over 90 % Ca and Mg recovery in seawater using NF, the process requires high pressure with tight pore membranes and only chloride-based salt separation is achieved, not hydroxide salts [23]. Likewise, chemical precipitation can easily separate Mg from seawater as $Mg(OH)_2$ with the addition of chemicals, but it is unable to recover Ca from seawater [12].

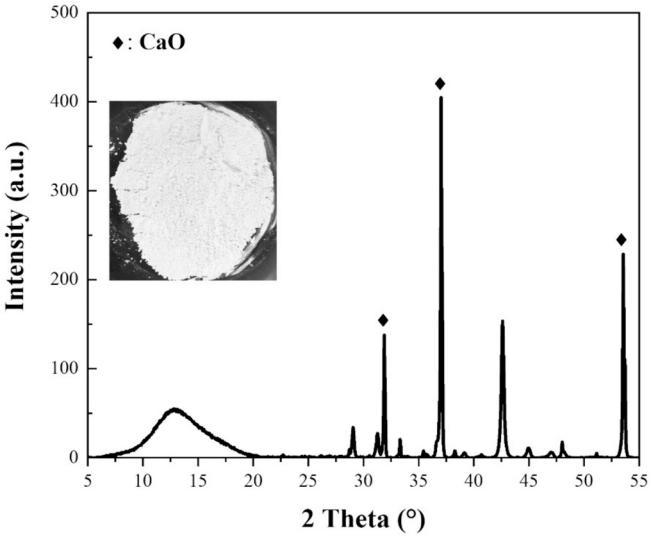

Fig. 10. XRD patterns of CaO (cement material) produced from seawater.

4. Conclusions

The current practice of cement production, which involves the calcination of limestone ($CaCO_3$), is a significant contributor to global carbon emissions. It is imperative to develop a cement production method that can substantially reduce CO_2 emissions. This study investigates a viable alternative pathway for generating raw materials essential for cement production, i.e., CaO and MgO, using a facile membrane electrolysis of seawater. We explored the potential use of a UF membrane as a simple, cost-effective and durable substitute for the AEM. Key findings include:

(i) Membrane electrolysis using a UF membrane exhibited performance comparable to that using an AEM, effectively producing hydroxide ions and facilitating the precipitation of Ca^{2+} and Mg^{2+}.
(ii) AEM allowed 51 % of Cl^- ions to migrate to the anode, twice the rate of the UF membrane, due to its electrostatic attraction and higher affinity for Cl^-. Both membranes facilitated 25–31 % migration of SO_4^{2-} ions.
(iii) The role of membrane is crucial for maintaining charge balance and providing OH^- for salt formation while preventing neutralization, as evident from the membrane-less ED experiment.
(iv) Both membranes achieved 97–99 % removal of Mg^{2+} and Ca^{2+} within 3 h, with insignificant changes to the membrane condition after one cycle. Repeated membrane reuse (3 cycles) resulted in membrane surface discoloration due to chloride oxidation with AEM exhibiting more severe oxidation effect.
(v) Using a Na_2SO_4 solution required an additional 20 mins to achieve similar removal efficiencies but offered cost advantages and selective separation of Mg^{2+} over Ca^{2+} compared to PBS solution.
(vi) The treated seawater is conducive to Li^+ recovery, attributable to 99 % removal of Mg^{2+} while maintaining insignificant Li^+ removal and the resultant alkaline environment (pH increased from 8.0 to 13.0), which is a favorable condition for Li^+ recovery using Li^+ ion sieves.
(vii) The membrane electrolysis process yielded precursors for MgO and CaO as byproducts, directly usable as cement material. This approach to recover Mg^{2+} and Ca^{2+} from seawater provides a more sustainable solution with substantially reduced carbon emissions in cement production compared to conventional cement production.

Given the favorable outcomes in this study using UF membranes, we suggest extending our research by exploring the potential application of more affordable, larger-pored commercial thin film composite membrane such as microfilter (MF) membranes as it could yield valuable insights into the scalability and cost-effectiveness of membrane electrolysis processes.

CRediT authorship contribution statement

Qian Chen: Writing – original draft, Methodology, Investigation, Formal analysis. **Youngwoo Choo:** Writing – review & editing, Validation, Data curation. **Nawshad Akther:** Writing – review & editing. **Ho Kyong Shon:** Writing – review & editing, Validation, Project administration. **Gayathri Naidu:** Writing – review & editing, Visualization, Supervision, Funding acquisition, Conceptualization.

Declaration of competing interest

The authors declare that they have no known competing financial interests or personal relationships that could have appeared to influence the work reported in this paper.

Data availability

No data was used for the research described in the article.

Acknowledgements

This research was supported by the Australian Research Council Discovery Early Career Research Award (DE200100661), ARC Discovery Projects (DP230100238); Johnson&Johnson WiSTEM Fellowship; and Australian-Indian Strategic Research Funding (AIRXII000019).

Appendix A. Supplementary data

Supplementary data to this article can be found online at https://doi.org/10.1016/j.cej.2024.153007.

References

[1] J. Deja, A. Uliasz-Bochenczyk, E. Mokrzycki, CO_2 emissions from Polish cement industry, Int. J. Greenhouse Gas Control 4 (2010) 583–588.
[2] V. Rahhal, R. Talero, Early hydration of portland cement with crystalline mineral additions, Cem. Concr. Res. 35 (2005) 1285–1291.
[3] R.M. Andrew, Global CO_2 emissions from cement production, Earth Syst. Sci. Data 10 (2018) 195–217.
[4] L.D. Ellis, A.F. Badel, M.L. Chiang, R.-J.-Y. Park, Y.-M. Chiang, Toward electrochemical synthesis of cement—an electrolyzer-based process for decarbonating $CaCO_3$ while producing useful gas streams, Proc. Natl. Acad. Sci. 117 (2020) 12584–12591.
[5] R. Snellings, Assessingunderstanding and unlocking supplementary cementitious materials, RILEM Technical Lett. 1 (2016) 50–55.
[6] A. Hasanbeigi, L. Price, E. Lin, Emerging energy-efficiency and CO_2 emission-reduction technologies for cement and concrete production: a technical review, Renew. Sustain. Energy Rev. 16 (2012) 6220–6238.
[7] C. Chen, G. Habert, Y. Bouzidi, A. Jullien, Environmental impact of cement production: detail of the different processes and cement plant variability evaluation, J. Clean. Prod. 18 (2010) 478–485.
[8] M.S. Imbabi, C. Carrigan, S. McKenna, Trends and developments in green cement and concrete technology, Int. J. Sustain. Built Environ. 1 (2012) 194–216.
[9] X.-J. Pan, Z.-H. Dou, T.-A. Zhang, D.-L. Meng, Y.-Y. Fan, Separation of metal ions and resource utilization of magnesium from saline lake brine by membrane electrolysis, Sep. Purif. Technol. 251 (2020) 117316.
[10] Y. Sano, Y. Hao, F. Kuwahara, Development of an electrolysis based system to continuously recover magnesium from seawater, Heliyon 4 (2018).
[11] C.H. Díaz Nieto, N.A. Palacios, K. Verbeeck, A. Prévoteau, K. Rabaey, V. Flexer, Membrane electrolysis for the removal of Mg^{2+} and Ca^{2+} from lithium rich brines, Water Res. 154 (2019) 117–124.
[12] A. Kumar, G. Naidu, H. Fukuda, F. Du, S. Vigneswaran, E. Drioli, J.H.V. Lienhard, Metals Recovery from Seawater Desalination Brines: Technologies, Opportunities, and Challenges, ACS Sustain. Chemi. Eng. 9 (2021) 7704–7712.
[13] S. Roobavannan, S. Vigneswaran, G. Naidu, Enhancing the performance of membrane distillation and ion-exchange manganese oxide for recovery of water and lithium from seawater, Chem. Eng. J. 396 (2020) 125386.
[14] E.J. Park, C.G. Arges, H. Xu, Y.S. Kim, Membrane strategies for water electrolysis, ACS Energy Lett. 7 (2022) 3447–3457.
[15] S. Ma, F. Yang, X. Chen, C.M. Khor, B. Jung, A. Iddya, G. Sant, D. Jassby, Removal of As(III) by electrically conducting ultrafiltration membranes, Water Res. 204 (2021) 117592.
[16] X. Zhou, L. Shi, R.F. Taylor, C. Xie, B. Bian, C. Picioreanu, B.E. Logan, Relative insignificance of polyamide layer selectivity for seawater electrolysis applications, Environ. Sci. Tech. 57 (2023) 14569–14578.
[17] A.S. Gangrade, S. Cassegrain, P. Chandra Ghosh, S. Holdcroft, Permselectivity of ionene-based, Aemion® anion exchange membranes, J. Membr. Sci. 641 (2022) 119917.
[18] E. Abdulkarem, Y. Ibrahim, V. Naddeo, F. Banat, S.W. Hasan, Development of Polyethersulfone/α-Zirconium phosphate (PES/α-ZrP) flat-sheet nanocomposite ultrafiltration membranes, Chem. Eng. Res. Des. 161 (2020) 206–217.
[19] K. Yang, I.M. Abu-Reesh, Z. He, Removal of disinfection byproducts through integrated adsorption and reductive degradation in a membrane-less electrochemical system, Water Res. 244 (2023) 120519.
[20] L. Semerjian, G. Ayoub, High-pH–magnesium coagulation–flocculation in wastewater treatment, Adv. Environ. Res. 7 (2003) 389–403.
[21] X. Huang, T. Wu, Y. Li, D. Sun, G. Zhang, Y. Wang, G. Wang, M. Zhang, Removal of petroleum sulfonate from aqueous solutions using freshly generated magnesium hydroxide, J. Hazard. Mater. 219 (2012) 82–88.
[22] S. Roobavannan, Y. Choo, D.S. Han, H.K. Shon, G. Naidu, Seawater lithium mining by zeolitic imidazolate framework encapsulated manganese oxide ion sieve nanomaterial, Chem. Eng. J. 474 (2023) 145957.
[23] H.-Z. Zhang, Z.-L. Xu, H. Ding, Y.-J. Tang, Positively charged capillary nanofiltration membrane with high rejection for Mg^{2+} and Ca^{2+} and good separation for Mg^{2+} and Li^{+}, Desalination 420 (2017) 158–166.